Steerable Balloon Endoscopes for Transcatheter Intracardiac Procedures

Max McCandless, Silvan Otto, and Pierre E. Dupont

Boston Children's Hospital, Harvard Medical School
max.mccandless@childrens.harvard.edu, pierre.dupont@childrens.harvard.edu

INTRODUCTION

While the repair and replacement of heart valves previously required the risk and trauma of open-heart surgery, transcatheter procedures and devices are rapidly developing as low-risk low-trauma alternatives [1]. A continuing challenge in the development of these techniques is the lack of direct visualization of valve tissue as is possible in open surgery. The standard catheter imaging modalities are fluoroscopy and ultrasound. Fluoroscopy enables visualization of the catheter, but not the tissue. Ultrasound images both the catheter and the tissue, but provides very noisy images.

To fill this imaging gap, cardioscopy (endoscopy inside the blood-filled heart) has been developed as a means of providing detailed visualization of the contact region between the catheter tip and the valve tissue [2]. Furthermore, cardioscopic imaging can enable autonomous robotic catheter procedures as demonstrated in [3].

Cardioscopes use an optically-clear "cap" or optical window on the imaging element. When the optical window is in the blood pool, the cardioscopic image is completely red, but when placed in contact with tissue, the optical window displaces the blood and so enables imaging of the contacting tissue.

When designing the optical window, the diameter of its distal face is a critical parameter since it determines the diameter of the cardioscopic field of view. The field of view diameter needs to be large enough to be able to identify what the catheter tip is touching inside the heart. For many applications, the minimum diameter for localization is 1cm.

Prior cardioscopes designed for valve repair used solid optical windows, which had to be inserted through the heart wall since their 1cm diameter was too large to introduce through the vasculature. For percutaneous access, an ideal optical window design should be collapsible during introduction into the vasculature, but capable of expansion once positioned inside the heart.

Saline-filled optically-clear balloons represent a promising approach which is explored in this paper. A prototype cardioscope balloon is depicted in Fig. 1. In this design, the distal tail of the balloon is inverted and glued to the tube forming the working channel so as to create a smooth distal surface on the optical window.

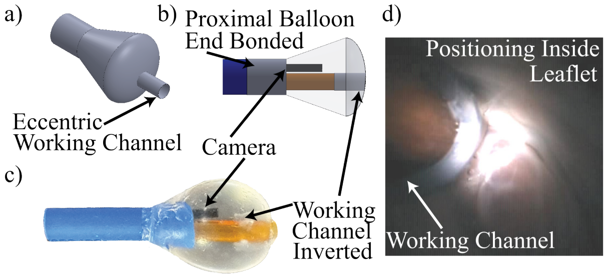

Fig. 1 Balloon cardioscope prototype. (a) Balloon schematic. (b) Cardioscope schematic. (c) Prototype. (d) Image of ex vivo aortic valve leaflet.

A chip camera with integrated LEDs for illumination is positioned inside the balloon. Since the working channel appears within the field of view (Fig. 1(d)), the cardioscope makes it possible to visualize the precise location of the working channel on heart valve tissue. This eccentric working channel differentiates the cardioscope from past works that are capable of observing and evaluating tissue, but not performing tissue modification [4].

Using existing technology, positioning the working channel inside the heart involves delivering the cardioscope using one or more telescoping steerable sheaths. Since these sheaths are ~1m long and contact vascular and cardiac tissue over much of their length, precise motions of the tip based on sheath bending can be challenging.

This paper investigates an alternative approach to fine positioning of the working channel which is based on building flexural degrees of freedom into the cardiocopic balloon. We demonstrate a balloon design in which inflation to an initial pressure fully inflates the optical window. Increases in pressure from this value produce flexure of the cardioscope while maintaining the original diameter of the optical window.

MATERIALS AND METHODS

We fabricated a steerable balloon prototype (30mm long, 4.62mm diameter uninflated) which consists of a 10mm long optical window and a 15mm long steerable section (as shown in Fig. 2). To achieve optical clarity, the balloon was made from Ecoflex™ 00-45 Near Clear™ using a 3D printed mold. The parameters $\{t_1, \ldots, t_5\}$, given in the caption of Fig. 2, were selected to decouple as much as possible window inflation and deflection by promoting

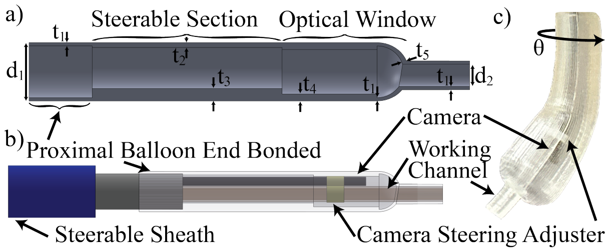

Fig. 2 Steerable balloon. (a) Balloon schematic showing design parameters. Selected values are: ($t_1 = 0.269$mm, $t_2 = 0.396$mm, $t_3 = 2.5t_1$, $t_4 = \frac{t_1+t_2}{2}$, $t_5 = 1.5t_1$, $d_1 = 4.62$mm, and $d_2 = 1.75$mm). (b) Cardioscope schematic. (c) Partially inflated prototype.

expansion of the balloon in a sequence prespecified by the differing thicknesses of the cross sections (thinner sections of the balloon expand first). While t_1 is minimized to allow for the proximal tube to be bonded to the base of the balloon and t_2 is set to ensure the camera and working channel fit through the balloon, $\{t_3, t_4, t_5\}$ are designed such that the optical window expands first, then the steering section bends toward the thicker internal diameter t_3 (toward the eccentric working channel). The design specifications were to obtain an optical window diameter of 10mm and a maximum bending angle of at least $\alpha_{\max} \geq 45°$. By rotating the cardioscope by an angle θ about its axis, a trumpet-shaped workspace can be produced.

The proximal end of the balloon is glued (Sil-Poxy™) to a 3.83mm tube through which is passed a 1mm diameter optical system (Myriad Fiber Imaging). The distal balloon tail is glued to a working channel tube. For purposes of rapid iteration, the distal tail is not inverted onto the working channel tube. The optical system is attached to the working channel by a clip (camera steering adjuster) which causes the optical system to follow the deflection of the working channel as the balloon steers the system. (Fig. 2(c)).

RESULTS

Experiments were conducted to characterize the steerable balloon's ability to independently inflate its optical window and to deflect based on inflation volume. Furthermore, tests were conducted to assess its workspace in terms of bending angle and with respect to imaging of the aortic valve.

A. Independence of Balloon Inflation and Deflection: Fig. 3 depicts optical window diameter and balloon deflection angle as functions of inflation volume. While window expansion occurs over the volume range of 3.7 to 5.7mL, balloon deflection occurs for higher inflation volumes. Successful decoupling of the DOFs is highlighted by the verticle green lines in the plot. The intended 10mm optical window diameter is achieved through the first portion of the bending from Fig. 3,(a)-(c) while bending occurs (Fig. 3(c)-(d)) as the balloon face diameter plateaus.

B. Workspace Validation: Fig. 4 illustrates the ability of the cardioscope to enhance the reachable workspace of a catheter system by making the balloon tip steerable. Fig. 4(a) illustrates the trumpet-shaped workspace obtained by inflating and rotating the cardioscope. Fig. 4(b) demonstrates how a steerable sheath approaching the aortic valve can be used to position the cardioscope over a desired leaflet while the steerability of the cardioscope can be used to control its orientation with respect to the leaflet.

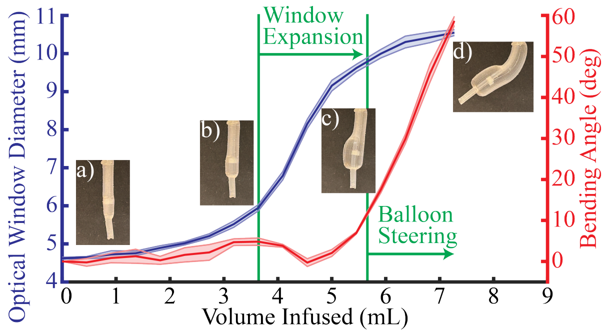

Fig. 3 Optical window diameter and bending angle as functions of inflation volume. Window expansion occurs over range of 3.7-5.7mL while bending up to 60° occurs over range of 5.7-7mL. (a-d) depict cardioscope at different inflation volumes.

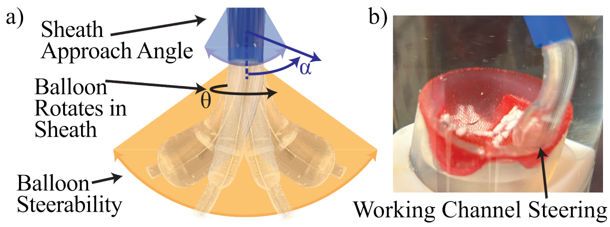

Fig. 4 Workspace validation experiment. (a) Cardioscope achieves trumpet-shaped workspace via combined inflation and rotation. (b) Cardioscopic degrees of freedom enable control of orientation for imaging desired aortic leaflet in phantom model.

DISCUSSION

Steerable balloon cardioscopes offer two advantages over prior designs. First, their collapsibility enables them to be introduced, e.g., transfemorally instead of through the heart wall. Second, their steerablity introduces an orientational degree of freedom without requiring an additional steerable sheath.

While space does not allow for in-depth design details here, the parameterized balloon model of Fig. 2(a) is highly adaptable by modifying cross sectional parameters to control optical window and working channel diameters as well as bending angle range. This can enable robotic catheter designs in which tendon-actuated sheaths are used for tip positioning while cardioscopic balloons control tip orientation.

ACKNOWLEDGEMENTS

This work was supported by NIH R01HL124020 and Max McCandless was supported by NIH T32HL007572.

REFERENCES

[1] A. Harky *et al.*, "The Future of Open Heart Surgery in the Era of Robotic and Minimal Surgical Interventions," *Heart, Lung and Circulation*, vol. 29, no. 1, pp. 49-61, 2020.

[2] B. Rosa, *et al.*, "Cardioscopically Guided Beating Heart Surgery: Paravalvular Leak Repair," *The Annals of Thoracic Surgery*, vol. 104, no. 3, pp. 1074-1079, 2017.

[3] G. Fagogenis, *et al.*, "Autonomous Robotic Intracardiac Catheter Navigation Using Haptic Vision," *Sci Robot.*, vol. 4, no. 29, 2019.

[4] Y. Uchida, *et al.*, "Recent Advances in Percutaneous Cardioscopy," *Curr Cardiovasc Imaging Rep*, vol. 4, pp. 317-327, 2011.